Role of claudin species–specific dynamics in reconstitution and remodeling of the zonula occludens

Yuji Yamazaki[a,*], Reitaro Tokumasu[a,*], Hiroshi Kimura[b], and Sachiko Tsukita[a]
[a]Laboratory of Biological Science, Graduate School of Frontier Biosciences and Graduate School of Medicine and
[b]Nuclear Dynamics Group, Graduate School of Frontier Biosciences, Osaka University, Osaka 565-0871, Japan

ABSTRACT **Tight-junction strands, which are organized into the beltlike cell–cell adhesive structure called the zonula occludens (TJ), create the paracellular permselective barrier in epithelial cells. The TJ is constructed on the basis of the zonula adherens (AJ) by polymerized claudins in a process mediated by ZO-1/2, but whether the 24 individual claudin family members play different roles at the TJ is unclear. Here we established a cell system for examining the polymerization of individual claudins in the presence of ZO-1/2 using an epithelial-like cell line, SF7, which lacked endogenous TJs and expressed no claudin but claudin-12 in immunofluorescence and real-time PCR assays. In stable SF7-derived lines, exogenous claudin-7, -14, or -19, but no other claudins, individually reconstituted TJs, each with a distinct TJ-strand pattern, as revealed by freeze-fracture analyses. Fluorescence recovery after photobleaching (FRAP) analyses of the claudin dynamics in these and other epithelial cells suggested that slow FRAP-recovery dynamics of claudins play a critical role in regulating their polymerization around AJs, which are loosely coupled with ZO-1/2, to form TJs. Furthermore, the distinct claudin stabilities in different cell types may help to understand how TJs regulate paracellular permeability by altering the paracellular flux and the paracellular ion permeability.**

Monitoring Editor
Keith E. Mostov
University of California, San Francisco

Received: Dec 23, 2010
Revised: Jan 31, 2011
Accepted: Feb 17, 2011

INTRODUCTION

The epithelial barrier is indispensable in multicellular organisms, in which it separates compositionally distinct fluid compartments. To form a transepithelial barrier between their apical and basal environments, epithelial cells first form a sheet via side-by-side cadherin-based cell–cell adhesions that create the beltlike adherens junction (AJ). Next, the AJ becomes a base for the polymerization of claudin proteins, which form the strands of the zonula occludens (beltlike tight junction [TJ]) to create the paracellular barrier (Tsukita *et al.*, 2001; Van Itallie and Anderson, 2006). The molecular basis of the spatiotemporally close relationship between the AJ and TJ has been intensely studied from various angles, focusing on adhesion molecules such as cadherins and claudins, scaffolding cytoskeletal elements, and cell-signaling molecules (Perez-Moreno *et al.*, 2003; Tsukita *et al.*, 2001; Schneeberger and Lynch, 2004; Gonzalez-Mariscal *et al.*, 2008; Nelson, 2009). The general consensus is that the hierarchical two-step formation of the AJ and TJ probably requires spatiotemporal regulation by signaling molecules that determine the adhesion molecules' organization in relation to cytoskeletal elements.

ZO-1/2/3 comprise a family of postsynaptic density 95/disc-large/zona occludens domain–containing membrane-scaffolding cytoskeletal proteins that bind to afadin and claudins, components of the AJ and TJ, respectively (Yamamoto *et al.*, 1997; Itoh *et al.*, 1999; Fanning and Anderson, 2009). They provide a cytoskeletal and signaling platform that regulates the construction of the AJs and TJs (Ikenouchi *et al.*, 2007; Yamazaki *et al.*, 2008). In this respect, an important recent finding is that ZO-1/2 determine where and when claudins are polymerized into TJ strands (Umeda *et al.*, 2006). In association with various kinds of adhesion molecules, transmembrane proteins, cytoskeletal components, and signaling molecules, ZO-1/2 play a dual role during the two-step formation of

This article was published online ahead of print in MBoC in Press (http://www.molbiolcell.org/cgi/doi/10.1091/mbc.E10-12-1003) on March 3, 2011.

*These authors contributed equally to this work.

Address correspondence to: Sachiko Tsukita (atsukita@biosci.med.osaka-u.ac.jp).

Abbreviations used: AJ, adherens junction; FF, freeze-fracture; FRAP, fluorescence recovery after photobleaching; GAPDH, glyceraldehyde-3-phosphate dehydrogenase; mAb, monoclonal antibody; MDCK, Madin-Darby canine kidney; pAb, polyclonal antibody; RT, reverse transcriptase; TJ, tight junction.

the AJ and TJ: They participate in the final establishment of the AJ and then play an indispensable role in the formation of the TJ by binding to and polymerizing claudins.

Recently evidence has accumulated that, rather than being uniform, the TJs display a wide variety of cell type–specific characteristics. One of the critical determinants of the properties of a TJ is thought to be the set of claudins that is expressed (Colegio *et al.*, 2002; Nitta *et al.*, 2003; Van Itallie *et al.*, 2003; Tamura *et al.*, 2011). The claudins comprise a multigene family of at least 24 members, which encode proteins containing four membrane-spanning domains (Tsukita *et al.*, 2001; Van Itallie and Anderson, 2006). The expression patterns of claudins in various cell types are complex. In most cells, multiple claudins are coexpressed, although in a few cases only one is expressed, for example, in Schwann cells, which express claudin-19, and in oligodendrocytes, which express claudin-11 (Gow *et al.*, 1999; Miyamoto *et al.*, 2005). This multiplicity makes sense as a way to create a large variety of claudin-dependent paracellular permselective barriers (Van Itallie and Anderson, 2006; Tsukita *et al.*, 2008). However, the molecular mechanisms that direct the claudins' polymerization and contribution to TJs in epithelial cells are not fully understood.

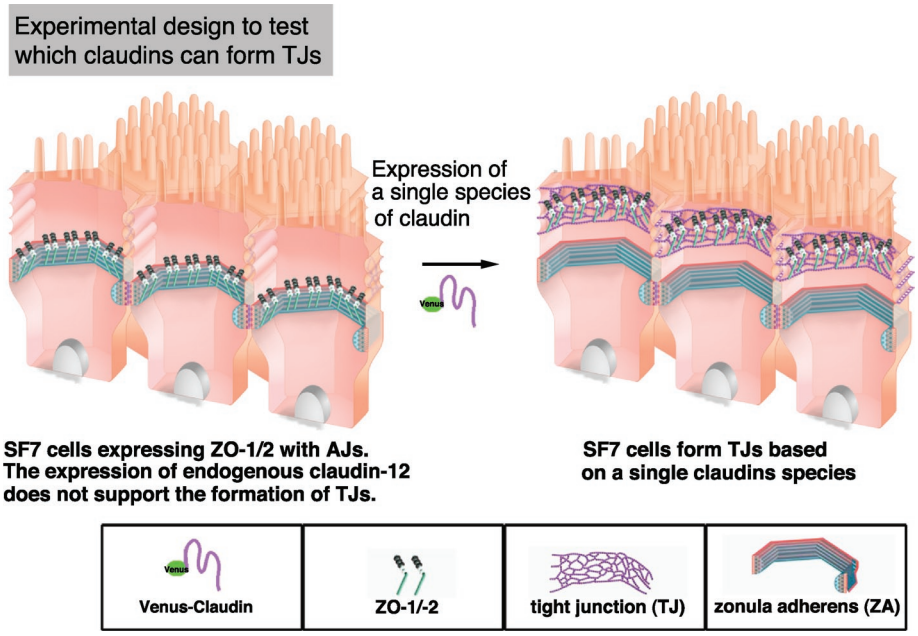

FIGURE 1: Experimental design for analyzing the ability of a single claudin species to polymerize to form TJs in epithelial cells. Epithelial-like cells in which beltlike AJs, but not beltlike TJs, are established without the endogenous expression of TJ-forming claudins provide a system for examining which claudin species can reconstitute the TJ upon their exogenous expression in the presence of ZO-1/2.

When exogenously expressed in nonepithelial cells, such as L cells, claudins polymerize, aberrantly forming claudin strands but not the beltlike TJs (Furuse *et al.*, 1998). However, this aberrant polymerization is typically inhibited in epithelial cells, where the specific polymerization of claudins is spatiotemporally permitted in the most apical region of the cell, just above the AJ (Claude and Goodenough, 1973). This specific polymerization in epithelial cells is considered to be attributable to and under the control of ZO-1/2, at least in part. Here we asked whether, in epithelial-like cells, the individual claudins polymerize on the AJ to form the TJ, under the control of ZO-1/2.

To answer this question, we established a simple model system using an epithelial-like cell line derived from testis, the SF7 cell line, which forms epithelial cell sheets that are free of TJs. We found by fluorescence recovery after photobleaching (FRAP) analyses that in SF7 epithelial cell sheets expressing a subset of claudins, the recovery dynamics of the TJ-forming claudins, claudin-7, -14, and -19, were slower than those of the other claudins, suggesting a close relationship between the FRAP dynamics of claudins and their ability to polymerize in the membrane to form TJs. Taking our results together with the results obtained in other types of epithelial cells, we propose that the individual dynamics of the different claudin species may be a critical parameter for determining the formation and remodeling of the TJ in epithelial cells in general.

RESULTS

An experimental system for reconstituting the TJ with a single claudin species

To examine the polymerization of every known claudin, we first looked for epithelial-type cells in which AJs, but no TJs, were established and that expressed ZO-1/2 but not claudins (Figure 1). Among the many cell lines examined, we found that the testis-derived SF7 cells had AJs but no TJs, as assessed by immunofluorescent staining for AJ and TJ markers, such as afadin and claudins/occludin, respectively, and by freeze-fracture (FF) images (Figure 2A and unpublished data). Real-time reverse transcriptase (RT)–PCR of the SF7 cells showed the expression of ZO-1/2 and occludin but not of tricellulin, another TJ component, and not of any claudins besides claudin-12 (Figure 2B). Although in the microarray analyses of SF7 cells, only claudin-9, claudin-12, and occludin, but not tricellulin, were detected (Supplementary Table S1), partly consistently with the real-time RT-PCR, no signals for claudin-9 or -12 were detected in immunoblots of SF7 cells. Furthermore, in the immunofluorescence, the signal for claudin-9 was barely detectable, and the signal for claudin-12 was weak, interrupted, and partly overlapping with ZO-1 in a dotted pattern. The signals from claudin-12 were visible in a dotted pattern at bi- and tricellular junctions (Supplemental Figure S1). Taken together with the results that exogenously expressed Venus–claudin-12 did not associate with ZO-1 but was diffusely expressed in the plasma membrane of SF7 cells, these observations indicated that even if claudin-12 was expressed in SF7 cells, only a small portion of it was arbitrarily colocalized with ZO-1, and it did not form TJs. In addition, occludin was not detected by immunofluorescence (Figure 2), consistent with the absence of TJs, because occludin is usually integrated into TJs.

These findings collectively indicated that the SF7 cells, without any TJ constitution, were a good model system to reconstitute TJs by the polymerization of exogenously expressed individual claudins. We therefore transfected these cells with a Venus-tagged form of each claudin and established stable clones. To reconstitute TJs, we carefully followed the procedure for cell-sheet formation. After the cells reached full confluence, forskolin was added to the culture medium to force the junctional configuration into straight-line segments (Fukuhara *et al.*, 2005). Six hours after the addition of forskolin, we examined the cells for the formation of TJs.

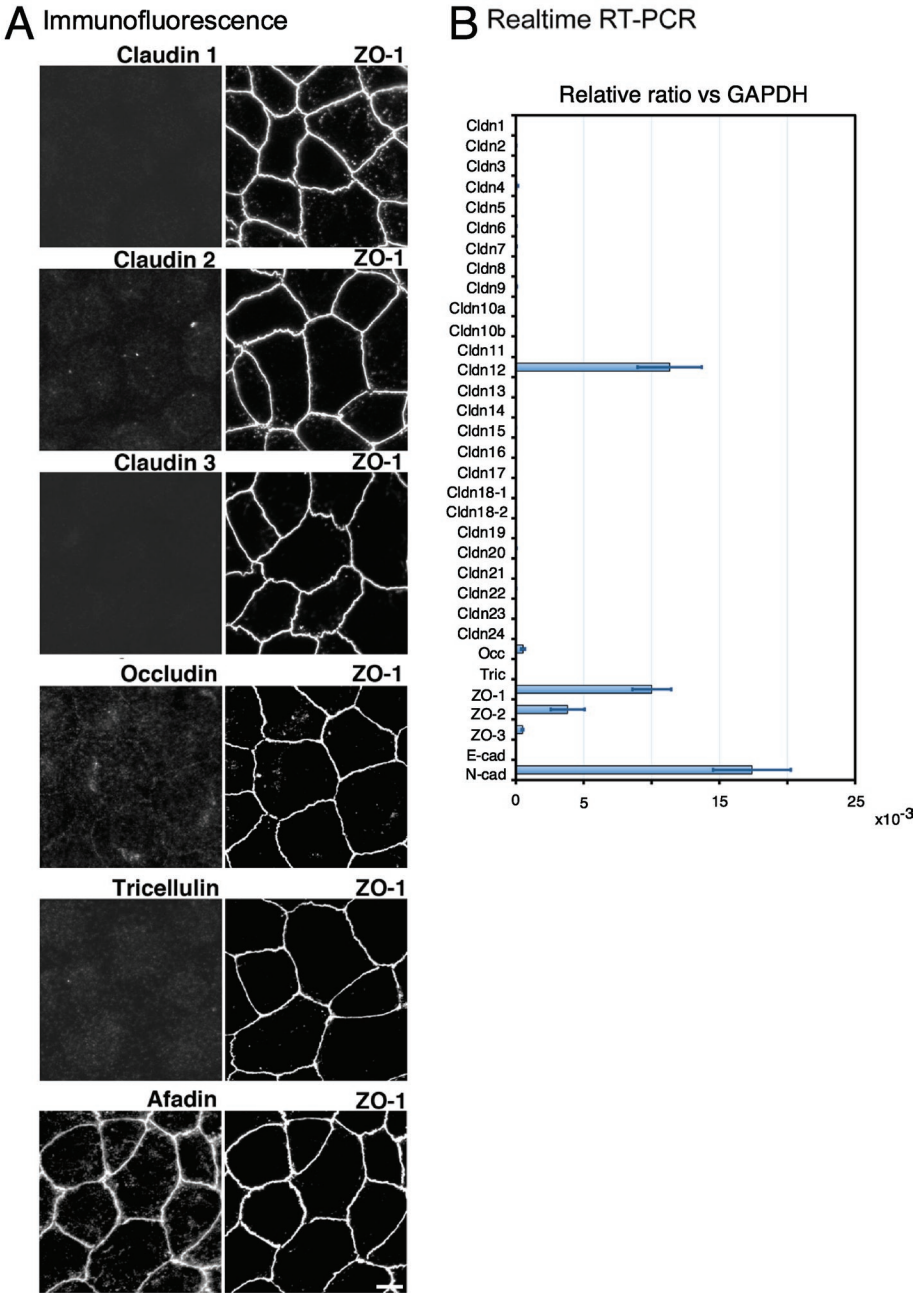

FIGURE 2: AJ- and TJ-related protein expressions in the epithelial-like cell line SF7. (A) Immunofluorescence of AJ- and TJ-related proteins in SF7 cells. Although ZO-1 was distributed in a polygonal pattern, none of the claudins were detected. The signals for occludin and tricellulin were barely detectable, even though occludin was amplified by real-time PCR. Afadin overlapped with ZO-1, indicating that the beltlike AJ had formed. Bar, 10 μm. (B) Real-time PCR analysis of AJ- and TJ-related genes. Among the 24 claudin genes, only claudin-12 was detected in the SF7 cells. Very low levels of occludin were detectable.

Three claudins—7, 14, and 19—polymerized on AJs to form TJ strands in stable SF7 transfectants, as revealed by immunofluorescence and FF electron microscopy

ZO-1 and afadin staining of the SF7 cells revealed that AJs were established during formation of the cell-sheet configuration (Figure 2A). We next introduced expression vectors for each Venus-claudin species and examined whether individual claudins could polymerize to form TJs in a ZO-1/2–dependent manner. Among the 24 claudins expressed in the SF7 transient transfectants, the signals for Venus-tagged claudin-1, -7, -10, -11, -14, -15, -19, and -20 were arranged linearly between cells and colocalized with the ZO-1 staining, but only the expressions of claudin-7, -10, -14, and -19 were maintained during the establishment of stable transfectants (Figure 3A and unpublished data). None of the junctional proteins were altered by the exogenous expression of the claudins on immunoblots, as far as we examined (Figure 3B).

Under FF electron microscopy, TJ strands were detected in the stable transfectants expressing claudin-7, -14, or -19 (Figure 4), but not in the one expressing claudin-10. For the immunoreplica method developed by Fujimoto *et al.* (1996), each claudin strand was specifically labeled by anti-GFP antibodies (Figure 4). Notably, the FF pattern of each claudin-based TJ strand was distinct, consistent with previous studies (Furuse *et al.*, 1999). Here we found that the epithelial-type beltlike TJ strands were first reconstituted by claudins. These results suggested that the specific claudin itself is a critical factor in determining the configuration of the TJ built on the AJ. Although claudin-10 colocalized with ZO-1, the FF replicas showed that it did not reconstitute TJ strands, indicating that some claudin species that were enriched in the junctions of stable transfectants and colocalized with ZO-1 could form TJs from TJ strands, and some could not.

Next, to examine the role of ZO-1/2 in the formation of the TJ strands, we transfected SF7 cells with Venus-tagged mutants of claudin-7, -10, -14, or -19, in which the ZO-1/2–binding regions were deleted. These claudins did not colocalize with ZO-1/2 in the cells, suggesting that ZO-1 plays a critical role in TJ formation (Supplemental Figure S2). Instead, the claudin mutants showed aberrant, non–belt-associated polymerization that was independent of ZO-1 (Supplemental Figure S3).

Although stable cell lines expressing claudin-1, -11, -15, or -20 were not established, these molecules colocalized with ZO-1/2 in transient transfectants, suggesting that these species might transiently form TJ strands. However, our FF analyses did not detect TJ strands in these cells, and we did not examine this possibility further for these claudin species. The claudins other than claudin-1, -7, -10, -11, -14, -15, -19, and -20 were expressed in the lateral membrane and did not colocalize with ZO-1/2. For these claudin species, we did not detect any TJ strands in the replica images, suggesting that they do not form TJs in the lateral membrane.

Collectively these findings showed that some single species of claudins polymerized to form TJ strands in the epithelial-like SF7 cells. This confirmed the previously proposed idea that claudins are

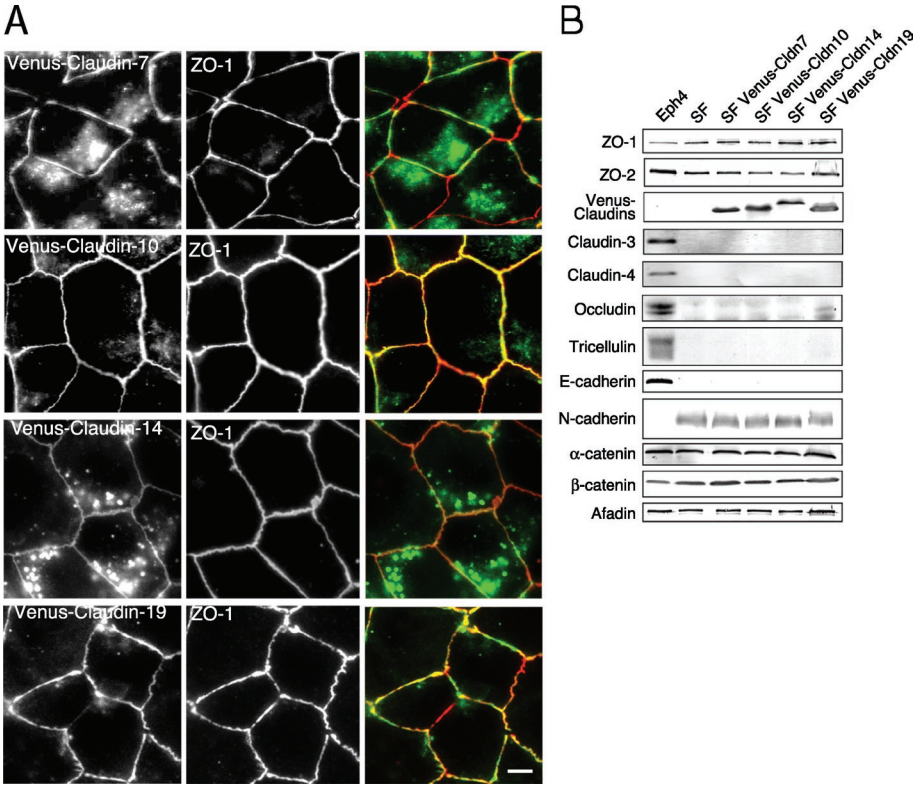

FIGURE 3: Three claudin species formed TJ strands colocalized with the beltlike patterns of ZO-1. (A) Immunofluorescence of Venus-claudin expressed in SF7 cells. The signal of four Venus-claudin species overlapped with the ZO-1 staining in single claudin–based TJs. Among them, Venus–claudin-7, -10, -14, or -19 stably formed TJ strands. Green: Venus, red: ZO-1, bar: 10 μm. (B) Immunoblotting for TJ- and AJ-related proteins. None of the stably transfected single claudin species caused changes in other AJ- or TJ-related proteins. Eph4 cells were examined as a typical epithelial cell.

required and sufficient to form the TJ under the control of ZO-1/2 and led to the question of what determines the ability of claudins to polymerize. It was previously reported that the FRAP dynamics between ZO-1 and claudin-1 are different in Madin-Darby canine kidney (MDCK) cells in which mixtures of claudin species are endogenously expressed (Shen *et al.*, 2008). Therefore we next examined the FRAP dynamics of single claudin species in stable transfectants as a possible determinant of each claudin's ability to polymerize to form TJs.

FRAP analysis of the dynamics of specific claudin species in relation to their ability to polymerize to form TJs

We first examined FRAP dynamics in single species–based TJs in SF7 cells stably expressing Venus-tagged claudin-7, -10, -14, or -19. After the transfectants were cultured on glass-bottomed dishes to form uniform confluent epithelial cell sheets, the linear signals of Venus-tagged claudin at the ZO-1–positive cell–cell contacts were bleached by a laser, and the fluorescence recovery was observed at 1-s intervals. Among these claudins, claudin-10 showed the fastest recovery of fluorescence intensity. On the other hand, claudin-7's fluorescence was barely visible after 60 s. The recovery rates for claudin-14 and claudin-19 were in between (Figure 5, A and B).

Because similar results were obtained from the transient expression of these claudin constructs, we examined the other claudins (for which stable clones were not established) by transiently expressing them in SF7 cells. In contrast to claudin-7, -10, -14, and -19, the fluorescence of the other claudins, which did not colocalize with ZO-1, showed an extremely fast recovery rate. The data for claudin-3 are shown in Figure 5C as an example. The mobile fraction and $t_{1/2}$ were calculated for each claudin from the recovery curves of the FRAP data (Tables 1–3). Thus each claudin species has a distinct dynamic behavior. Furthermore, there was a clear correlation between the recovery rate in the FRAP analysis and the polymerization of the claudins. Claudin-7, -14, and -19 showed slow recovery rates, which probably enabled their polymerization to form TJ strands. The other species of claudin did not polymerize with more rapid FRAP dynamics. Claudin-10 exhibited what is likely to be a critical recovery rate, in which the claudin molecules were concentrated enough to merge with the linear cell–cell ZO-1 signals but not enough to be polymerized into TJ strands.

FRAP analysis of ZO-1 involved in cell–cell adhesion

Because ZO-1/2 are required for claudin polymerization, we investigated how the FRAP dynamics of membrane-scaffolding proteins such as ZO-1 affected TJ formation. We therefore examined the recovery dynamics of mCherry–ZO-1 proteins by FRAP analysis, how the rates were influenced by claudins, and whether these molecules formed a complex with claudins. The results showed that ZO-1 consistently had faster recovery rates than any of the claudins, and their dynamics were not affected by claudin polymerization (Figure 6). Taken together, these data indicated that the formation of TJ strands by claudin polymerization and the regulation of their polymerization by the membrane-scaffolding protein ZO-1 probably occur at the cell–cell junction in a specific manner that does not require the formation of a rigid complex. Hence the distinct dynamics of each claudin species may depend on its own traits, such as the thermodynamic properties of the claudin molecule itself as well as on claudin–claudin or claudin–membrane interactions in the presence of ZO-1/2.

Claudin dynamics and TJ formation differ in different epithelial cells

To assess whether the dynamics of the individual claudin species were constant in all epithelial cells, we performed the FRAP analysis in Eph4 cells, in which various claudin species were expressed as shown by real-time RT-PCR (Supplemental Figure S4). We found that Venus-tagged claudin-7, -10, -14, and -19, which were highly concentrated at the ZO-1–positive cell–cell contacts in SF7 cells, were also concentrated at cell–cell contacts in Eph4 cells. Venus-tagged claudin-3 and -12, which were not concentrated at ZO-1–positive cell–cell contacts in SF7 cells, were concentrated at them in Eph4 cells. On the other hand, the FRAP recovery rates of these claudins were relatively largely changed (for claudin-3, -7, -14, -19) or almost unchanged (for claudin-10) between SF7 and Eph4 cells. The recovery of claudin-3 in Eph4 cells was slower than in SF7 cells, with a rate similar to that of claudin-7, probably because claudin-3 was integrated into TJs in the Eph4 cells (Figure 7). The FRAP recovery dynamics of claudin-7, -14, and -19 were slow in the Eph4 cells,

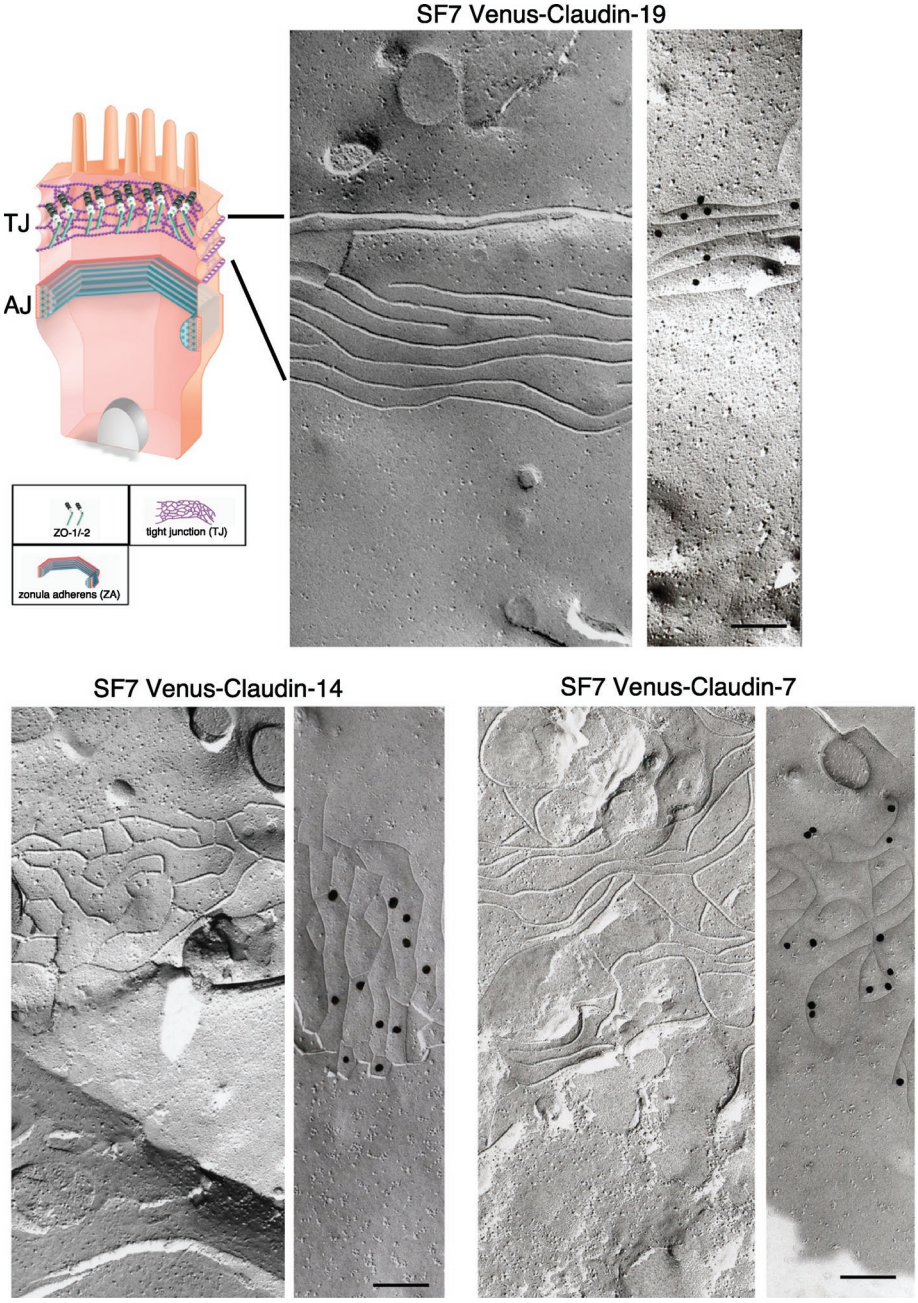

FIGURE 4: Different patterns of claudin strands derived from single claudin species. FF analysis of SF7 cells stably transfected with Venus-tagged claudin-7, -14, or -19. Top left, a schematic drawing of an epithelial cell. Each of these claudin species formed TJ strands, but with a different pattern, as shown in the FF replicas. Immunolabeling by the Fujimoto method showed that each strand was specifically labeled with gold particles. Each gold particle was 25 nm in diameter. Bar, 200 nm.

similar to those in SF7 cells, although their rank differed between these two cell lines. Thus the high stability that characterized claudin-7, -14, and -19 in SF7 cells, as demonstrated by their FRAP recovery dynamics, is probably required for the polymerization of other claudins in other epithelial cells, like Eph4 cells. The FRAP dynamics of claudin-10 were not effected by whether it was not integrated or integrated in SF7 and Eph4 cells, respectively.

The situation was different in MDCK I cells, where the transepithelial barrier function is very strong, presumably because of the high expression levels of endogenous claudins in these cells. However, we did not perform a thorough expression analysis of the endogenous canine claudins in MDCK I cells because we lacked the appropriate primers. All of the exogenously expressed claudins in this cell type were concentrated in the TJ. FRAP analyses of these TJs revealed that all of the claudin species except for claudin-12 showed relatively slow recovery times, comparable to those of the TJ-forming claudins in SF7 cells. On the other hand, the FRAP dynamics of claudin-10 and -12 were notable, being consistently faster than those of the other TJ-forming claudins in all the epithelial cells examined. These results indicated that claudin-10 and -12, which did not form TJs in SF7 cells, might be integrated into claudin strands with high dynamics in Eph4 and MDCK I cells, unlike the other types of claudins examined that showed stabilized FRAP dynamics. Taken together, these data confirmed that the regulation of claudin dynamics plays a critical role in inducing claudin polymerization to form TJs.

The effect of claudin phosphorylation on FRAP dynamics in Eph4 cells

The polymerizing claudins showed slower FRAP recovery dynamics than the nonpolymerizing ones, indicating that the molecular dynamics of the claudins is an important target for the regulation of claudin polymerization. Therefore we next examined whether a modification, such as phosphorylation, could regulate claudin polymerization. It was previously reported that T203 of claudin-1 is regulated by mitogen-activated protein kinase, and its phosphorylation modulates the transepithelial electrical resistance and solute flux via TJs (Fujibe *et al.*, 2004). To examine whether this phosphorylation is associated with claudin FRAP recovery dynamics, we performed FRAP analysis in Eph4 cells using Venus-phosphomimetic T203D–claudin-1 or Venus-dephosphomimetic T203A–claudin-1. Both of these constructs were localized to the TJs in Eph4 cells, similar to the wild-type construct. Moreover, the FRAP analysis indicated that the phosphorylation of claudin-1 on T203 did not affect its recovery time (Figure 7).

DISCUSSION

In the present study, we established a simple epithelial cell system to examine the ability of each type of claudin to polymerize to form the claudin-based TJ under the control of ZO-1/2 using SF7 cells, which are derived from testis. We looked for epithelial cell types in which no TJ was present, but this point was very difficult to confirm. First, we repeatedly analyzed the expressions of claudins, occludin, and tricellulin by real-time RT-PCR and then by immunoblotting and immunofluorescence. Then we checked the presence of TJ strands in FF replicas. Untransfected SF7 cells showed no TJ strands by immunofluorescence or in FF replicas, even though they expressed low

Cell type (transfection)	Cldn7	Cldn10	Cldn14	Cldn19	Cldn12	Cldn3
a. Mobile fraction (%)						
SF7 (stable)	9.4	65.4	27.7	23.5		
SF7 (transient)	12.2	52.8	31.7	27.4		60.9
MDCK I (stable)	17.5	37.4	13.9	12.5	51.9	12.5
Eph4 (transient)	26.8	51.8	12.4	17	52.9	34
b. $t_{1/2}$ (in s) of FRAP recovery						
SF7 (stable)	12.9	15.9	13.6	11.5		
SF7 (transient)	13.9	15.5	18.2	11.6		6
MDCK I (stable)	11.4	24.8	12.6	17.2	16.9	11.6
Eph4 (transient)	10.5	13.7	10.8	13.5	16.8	18.9

TABLE 1: Mobile fractions and $t_{1/2}$ of FRAP recovery observed in this study for various claudins in different lines.

Cell type (transfection)	Cldn7 (stable)	Cldn10 (stable)	Cldn14 (stable)	Cldn19 (stable)	Parental SF7
Mobile fraction (%)	31.8	35.3	35.9	45.3	39.9
$t_{1/2}$ (s)	12	14.3	12.9	12.6	19.2

TABLE 2: Mobile fractions and $t_{1/2}$ of FRAP recovery observed in this study for Cherry–ZO-1 in parental SF7 cells and claudin-expressed SF7 cells.

Cell type (transfection)	Cldn1	Cldn1 T207A	Cldn1 T207D
Mobile fraction (%)	24	23.8	23.3
$t_{1/2}$ (s)	14.7	12.8	12.4

TABLE 3: Mobile fractions and $t_{1/2}$ of FRAP recovery observed in this study for the mutants of Venus–claudin-1 in Eph4 cells.

levels of occludin and substantial levels of claudin-12. Other epithelial-type cells, such as 293 cells, and typical epithelial cells, like Eph4 and MDCK I cells, showed TJs by immunofluorescence for occludin and certain claudins, which we used for the initial screening.

In SF7 cells, three species of claudins polymerized to form TJs, and the others did not. These differences were at least partly due to differences reflected in their FRAP dynamics. As revealed by FRAP analysis, the polymerizing claudins showed significantly slower recovery dynamics than the nonpolymerizing ones. Thus the molecular dynamics of claudins offer an important target for regulating their polymerization, and factors that extracellularly or intracellularly modulate claudin dynamics could be regulators of TJ function. The modification of claudins, including their carboxylation or phosphorylation, the presence of claudin-interacting proteins such as ZO-1/2, and even the lipid composition of the membrane region with which ZO-1/2 are associated are candidates for such regulators. Although we did not detect any effects of the phosphorylation in the present study, the present analyses provide some insight into the regulation of TJ formation, which will be further explored in future studies.

The data on claudin polymerization in SF7 cells presented here revealed claudin-specific FRAP dynamics and an important correlation between these dynamics and the formation of TJs. Furthermore, when each claudin species was expressed in epithelial cells that contained preexisting TJs consisting of complexed claudins, the exogenous claudin was integrated into the preexisting TJs, while some claudins, such as claudin-10 or -12, retained their rapid dynamics in MDCK I and Eph4 cells. Thus complex interactions between different species of claudins had differential effects on their FRAP recovery rates, suggesting that they integrate into the TJs at different rates and affinities.

Current evidence suggests that claudins can be divided into two types, paracellular barrier forming and paracellular ion permeability forming (Tsukita and Furuse, 2000; Anderson and Van Itallie, 2009; Shen *et al.*, 2011), and distinct kinds of interactions are known to occur between them (Furuse *et al.*, 1999; Hou *et al.*, 2009, 2010). The ion permeability–forming claudins are ion-leaky claudins that permit selective permeability to ions (Van Itallie *et al.*, 2008; Tamura *et al.*, 2011). The specific combinations of barrier-forming and permeability-forming claudins are critical to determine tissue-specific functions of the TJs. In any case, the interactions between claudin molecules are a critical factor for TJ functioning, making the regulation of claudin expression important for the maintenance of the paracellular barrier in biological systems.

The ZO-1/2–dependent formation of the TJ plays a critical role in epithelial paracellular barrier functions, which we were unable to reconstitute in the present study. There are several possible reasons for this inability. Of course, the complex expression of several claudins might be required for the formation of stable TJs that have a paracellular barrier function, as discussed above. In addition, in contrast to Eph4 or other epithelial cell lines, the SF7 cells express N-cadherins. Although N-cadherin–based AJs exist in vivo, for example, in retinal pigment epithelium cells and hepatocytes, we cannot exclude the possibility that TJ dynamics interfere with the E-cadherin–based AJs in epithelial cells or the N-cadherin–based AJs in the SF7 cells.

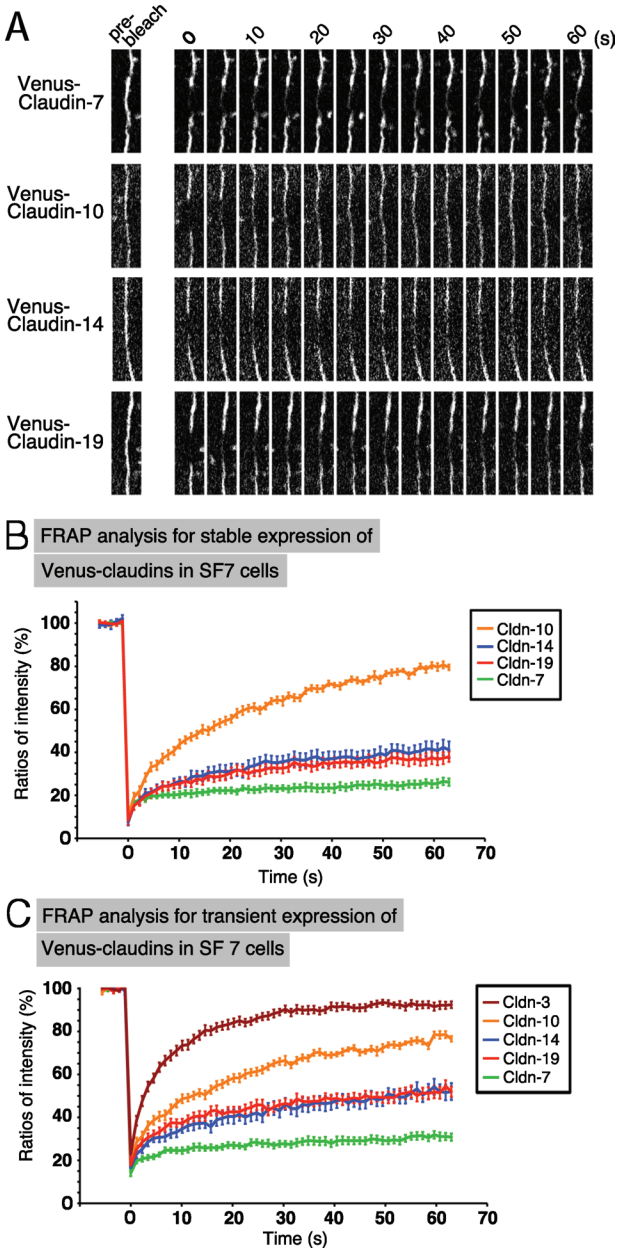

FIGURE 5: Individual claudins showed distinct FRAP dynamics in SF7 cells. (A) FRAP analysis of Venus–claudin-7, -10, -14, and -19 stably expressed in SF7 cells. High-magnification images of TJ segments at the indicated time points after photobleaching are shown. (B) Quantitative FRAP analysis in SF7 cells. FRAP analysis of Venus–claudin-7, -10, -14, and -19 stably expressed in SF7 cells. Different claudins had distinct behaviors in SF7 cells. The mobile fraction and $t_{1/2}$ of recovery for each protein are shown in Table 1. N ≥ 15 for each. (C) FRAP analysis of Venus–claudin-3, -7, -10, -14, and -19 transiently expressed in SF7 cells. Different claudins had distinct behaviors in SF7 cells. Claudin-3's recovery was significantly faster than that of the other claudins, and this claudin did not polymerize to form TJs in SF7 cells. The mobile fraction and $t_{1/2}$ of recovery for each protein are shown in Table 1. N ≥ 14 for each.

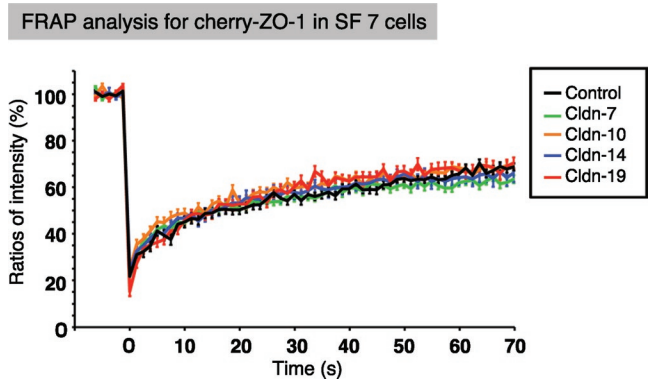

FIGURE 6: ZO-1 FRAP recovery rates are only loosely coupled with those of claudin strands in SF7 cells. Quantitative FRAP analysis for ZO-1 in SF7 cells and their single claudin–expressing transfectants. The mobile fraction and $t_{1/2}$ of recovery for each protein are shown in Table 2. There were no significant differences in the FRAP behavior of ZO-1 among the control SF7 cells and each transfectant. N ≥ 15 for each.

Second, we showed that occludin and tricellulin were rarely recruited to the cell–cell contacts in SF7 cells, even when claudin-7, -14, and -19 polymerized to form TJ strands. We considered the possibility that occludin and tricellulin were not autonomously integrated into the claudin strands but that their integration into the TJ was regulated by other kinds of claudins or by other signals and/or modifications. Recently several reports indicated that occludin and tricellulin may play a role in the signaling that regulates the paracellular barrier, rather than in the barrier's structural backbone (Marchiando *et al.*, 2010). In this respect, occludin-deficient mice show a complex but not lethal phenotype that might be related to the regulation of TJ function (Saitou *et al.*, 2000). The mechanism by which occludin or tricellulin is recruited to the TJ might be a point of regulation for paracellular barrier functioning.

In the ZO-1/2–dependent formation of the TJ, it was surprising that ZO-1/2 showed different dynamics from those of the claudins. In SF7 cells, the dynamics of ZO-1/2 were not influenced by the presence of TJs: That is, when the TJs contained claudin-7, -14, or -19, the ZO-1/2 dynamics were the same as in the parental SF7 cells. These results were partly consistent with previously reported findings using mixed expressions of claudins (Shen *et al.*, 2008; Yu *et al.*, 2010). This loose coupling between the claudins and ZO-1/2 is noteworthy. The critical mode of association between the claudins and ZO-1/2 remains a subject for future study.

There are at least two noteworthy points regarding the biological relevance of the dynamic characteristics of the claudins in the TJ. First, the slow FRAP-recovery dynamics promoted the claudins' accumulation around AJs by loose coupling between claudins and ZO-1/2, although the signals that regulate their dynamics remain to be studied. This concept of TJ regulation is a new one. Our novel assay system, described here, may be useful for studying the mechanism of the formation of TJs, which might provide new clinical applications. The second point regards the dynamics of claudins in the preformed TJ, which regulates paracellular permeability across epithelial cell sheets. Distinct claudin stabilities might also affect how TJs regulate paracellular permeability by altering the paracellular flux and the paracellular ion permeability. Thus the identification of factors that regulate claudin dynamics is challenging, but important. Studies along these lines are being conducted in our laboratory.

MATERIALS AND METHODS

Cell culture and staining

SF7 cells were kindly gifted from Takashi Shinohara (Kyoto University, Kyoto, Japan). SF7 cells are derived from testis (van der Wee and Hofmann, 1999). Eph4 and SF7 cells were cultured in DMEM containing 10% fetal calf serum. The cells were analyzed 6 h after

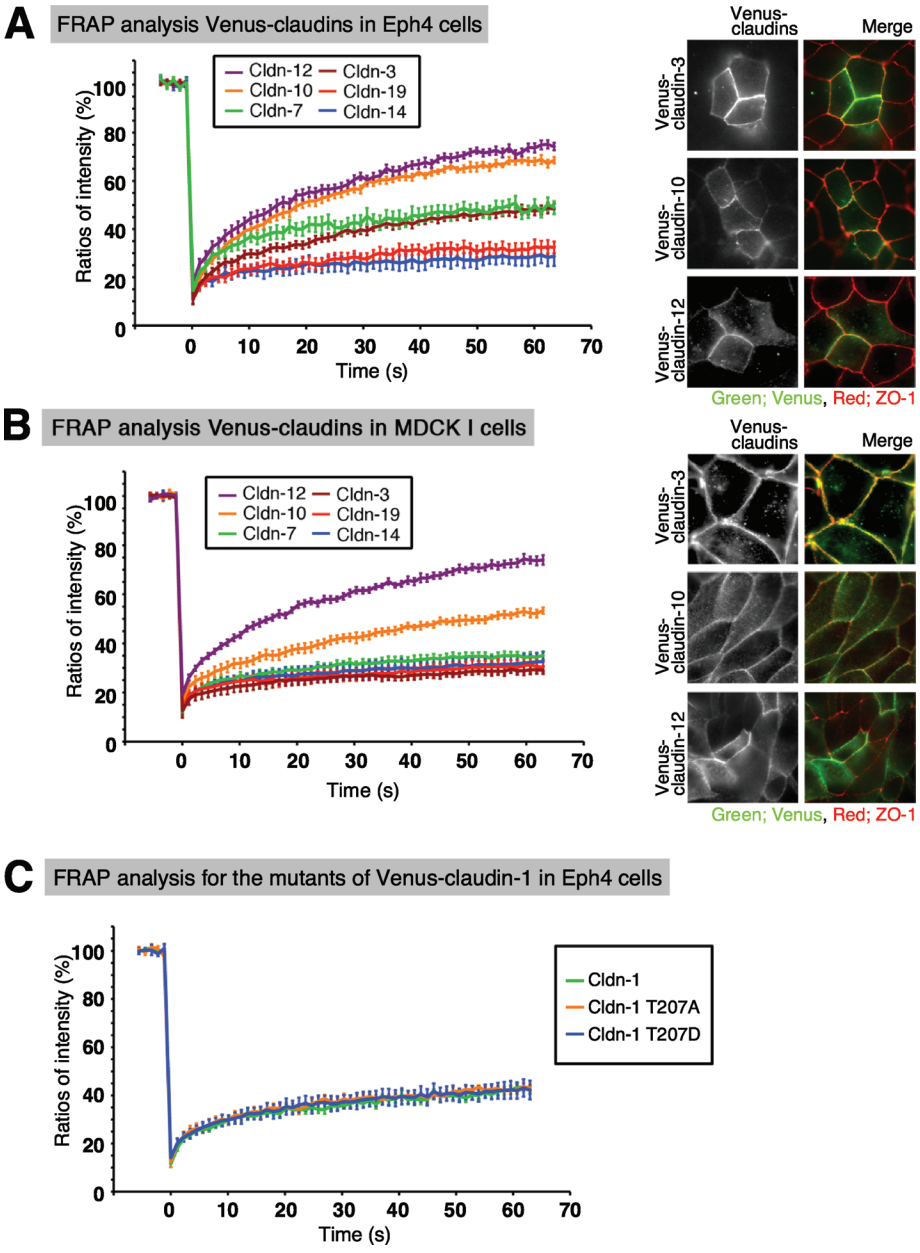

FIGURE 7: Individual claudins show different FRAP dynamics in Eph4 and MDCK I cells, typical epithelial cell lines. (A) Quantitative FRAP analyses of transiently expressed Venus-claudins in Eph4 cells. Distinct claudin behaviors were detected in Eph4 cells. The mobile fraction and $t_{1/2}$ of recovery for each protein are shown in Table 1. The recovery of claudin-3 was slower in Eph4 than in SF7 cells, suggesting that claudin-3 is polymerized in the Eph4 cells. Note that the dynamics of claudin-10 and -12 were faster than those of the other stabilized claudins. N ≥ 15 for each. Right, immunofluorescence images of Eph4 cells transiently expressing claudin-3, -10, or -12 are shown. Three of them colocalized with ZO-1 in Eph4 cells. Green: Venus, red: ZO-1. (B) Quantitative FRAP analyses of stably expressed Venus-claudins in MDCK I cells. The mobile fraction and $t_{1/2}$ of recovery for each protein are shown in Table 1. The recovery of claudin-3 was slower in MDCK I cells than in SF7 cells, suggesting claudin-3 is polymerized in the MDCK I cells. Compared with the results for Eph4 cells, the recovery of claudin-10 was more stable, but it was still distinct from the other stabilized claudins such as claudin-7. N ≥ 15 for each. Right, immunofluorescence images of Eph4 cells transiently expressing claudin-3, -10, or -12 are shown. Three of them colocalized with ZO-1 in Eph4 cells. Green: Venus, red: ZO-1. (C) Quantitative FRAP analyses of transiently expressed Venus-phosphomimetic or dephosphomimetic claudin-1 mutants in Eph4 cells. There were no significant differences in the FRAP dynamics of claudin-1 at different phosphorylation states. N ≥ 15 for each. The mobile fraction and $t_{1/2}$ of recovery for each protein are shown in Table 3.

forskolin (final 10 μM) was added. For immunofluorescence, the cells were fixed in iced methanol for 5 min. Immunostainings were performed as previously described (Yamazaki *et al.*, 2008).

Plasmids and constructions

Occludin, tricellulin, and all the claudins were generated by PCR and subcloned into the CAGGS–N-terminus–Venus vector. The mutants of claudin-1 were generated by site-directed mutagenesis and subcloned into the CAGGS–N-terminus–Venus vector. ZO-1 was subcloned into the CAGGS–N-terminus–mCherry vector.

Antibodies

Rabbit anti–claudin-9, -11, and -15 polyclonal antibodies (pAbs) were generated and characterized in Tsukita's laboratory. Rabbit anti–claudin-3 pAb and mouse anti–claudin-4 monoclonal antibody (mAb) were purchased from Invitrogen. Rabbit anti–claudin-12 pAb was from IBL (Gumma, Japan). Mouse anti–ZO-1 mAb, rat anti-occludin mAb (Moc37), rat anti-tricellulin mAb, rabbit anti–ZO-2 pAb, rabbit anti-afadin pAb, and rabbit anti–green fluorescent protein (GFP) pAb were generated and characterized in Tsukita's laboratory. Rat anti–mouse E-cadherin mAb (ECCD2) was generously provided by M. Takeichi (Riken, CDB, Kobe, Japan). Rabbit anti–β-catenin pAb and anti–α-catenin pAb were purchased from Sigma. Rabbit anti–N-cadherin pAb was purchased from Abcam (Cambridge, UK).

Electron microscopy

The transmission electron microscopy, the FF method, and the Fujimoto method for immunoreplication were performed as described previously (Fujimoto *et al.*, 1996; Umeda *et al.*, 2006).

FRAP analysis

FRAP was performed by confocal microscopy (LSM 510 META operated by software version 3.0, Carl Zeiss Microimaging) with a Plan-Neofluar 40× 1.3 numerical aperture oil immersion lens. A heated chamber (Tokai Hit) was used to keep the temperature at 37°C and maintain the CO_2 in the chamber at 5%. For the FRAP analysis of claudins, the images were collected with the following parameters: 512 × 128 pixels, zoom 5, scan speed 12, pinhole max airy unit, and 0.05% transmission of a 458 Ar laser with 60% output power. A targeted region was bleached using 100% transmission at 458, 488, and 514 nm (8 pulses). For the FRAP analysis of ZO-1, the

images were collected with the following parameters: 512 × 128 pixels, zoom 5, scan speed 12, pinhole max airy unit, and 40% transmission at 543 nm. A target region was bleached using 100% transmission at 488, 514, and 543 nm (10 pulses). After the fluorescence intensity of the bleached area was measured, the intensity was tracked and normalized to the initial intensity before bleaching using ImageJ software (National Institutes of Health, Bethesda, MD).

Quantitative real-time RT-PCR

Real-time PCR with SYBR Green technology was used to measure mRNA levels. The RNAs were reverse transcribed to cDNA by Superscript II RT. The sequences of specific primers are listed in Supplemental Table S1. Designed specific primers for all the claudins except for claudin-3 and claudin-22 were generated previously (Tamura *et al.*, 2008). The primers of occludin, ZOs, claudin-3, claudin-22, and tricellulin were generated in our laboratory. The primers for E-cadherin and N-cadherin were described previously (Wong *et al.*, 2000, Lindner *et al.*, 2010). We normalized the gene expression to the glyceraldehyde-3-phosphate dehydrogenase (GAPDH) expression by calculating the ΔCt = (Ct of GAPDH – Ct of gene). Setting the expression value of GAPDH to 1.0, the relative expression values were calculated as $2 \wedge \Delta Ct$.

Statistical analysis

At least three independent experiments were performed. All statistical analyses are indicated as mean ± standard error of the mean.

ACKNOWLEDGMENTS

We are grateful to Chiyomi Inoue, Yuka Miyake, and Chieko Hemmi for their technical assistance and Grace Gray and Leslie Miglietta for proofreading the manuscript. We further thank all the members of our laboratory, especially Atsushi Tamura, for helpful discussions. This study was supported in part by a Grant-in-Aid for Creative Scientific Research and for young scientists from the Ministry of Education, Science, and Culture of Japan to S.T. and Y.Y., respectively.

REFERENCES

Anderson JM, Van Itallie CM (2009). Physiology and function of the tight junction. Cold Spring Harb Perspect Biol 1, a002584.

Claude P, Goodenough DA (1973). Fracture faces of zonulae occludentes from "tight" and "leaky" epithelia. J Cell Biol 58, 390–400.

Colegio OR, Van Itallie CM, McCrea HJ, Rahner C, Anderson JM (2002). Claudins create charge-selective channels in the paracellular pathway between epithelial cells. Am J Physiol Cell Physiol 283, 142–147.

Fanning AS, Anderson JM (2009). Zonula occludens-1 and -2 are cytosolic scaffolds that regulate the assembly of cellular junctions. Ann NY Acad Sci 1165, 113–120.

Fujibe M, Chiba H, Kojima T, Soma T, Wada T, Yamashita T, Sawada N (2004). Thr203 of claudin-1, a putative phosphorylation site for MAP kinase, is required to promote the barrier function of tight junctions. Exp Cell Res 295, 36–47.

Fujimoto K, Umeda M, Fujimoto T (1996). Transmembrane phospholipid distribution revealed by freeze-fracture replica labeling. J Cell Sci 109, 2453–2460.

Fukuhara S, Sakurai A, Sano H, Yamagishi A, Somekawa S, Takakura N, Saito Y, Kangawa K, Mochizuki N (2005). Cyclic AMP potentiates vascular endothelial cadherin-mediated cell-cell contact to enhance endothelial barrier function through an Epac-Rap1 signaling pathway. Mol Cell Biol 25, 136–146.

Furuse M, Sasaki H, Fujimoto K, Tsukita S (1998). A single gene product, claudin-1 or -2, reconstitutes tight junction strands and recruits occludin in fibroblasts. J Cell Biol 143, 391–401.

Furuse M, Sasaki H, Tsukita S (1999). Manner of interaction of heterogeneous claudin species within and between tight junction strands. J Cell Biol 147, 891–903.

González-Mariscal L, Tapia R, Chamorro D (2008). Crosstalk of tight junction components with signaling pathways. Biochim Biophys Acta 1778, 729–756.

Gow A *et al.* (1999). CNS myelin and sertoli cell tight junction strands are absent in *Osp/claudin-11* null mice. Cell 99, 649–659.

Hou J, Renigunta A, Gomes AS, Hou M, Paul DL, Waldegger S, Goodenough DA (2009). Claudin-16 and claudin-19 interaction is required for their assembly into tight junctions and for renal reabsorption of magnesium. Proc Natl Acad Sci USA 106, 15350–15356.

Hou J, Renigunta A, Yang J, Waldegger S (2010). Claudin-4 forms paracellular chloride channel in the kidney and requires claudin-8 for tight junction localization. Proc Natl Acad Sci USA 107, 18010–18015.

Ikenouchi J, Umeda K, Tsukita S, Furuse M, Tsukita S (2007). Requirement of ZO-1 for the formation of belt-like adherens junctions during epithelial cell polarization. J Cell Biol 176, 779–786.

Itoh M, Furuse M, Morita K, Kubota K, Saitou M, Tsukita S (1999). Direct binding of three tight junction-associated MAGUKs, ZO-1, ZO-2, and ZO-3, with the COOH termini of claudins. J Cell Biol 147, 1351–1363.

Lindner I *et al.* (2010). α2-Macroglobulin inhibits the malignant properties of astrocytoma cells by impeding β-catenin signaling. Cancer Res 70, 277–287.

Marchiando AM *et al.* (2010). Caveolin-1-dependent occludin endocytosis is required for TNF-induced tight junction regulation. J Cell Biol 189, 111–126.

Miyamoto T *et al.* (2005). Tight junctions in Schwann cells of peripheral myelinated axons: a lesson from claudin-19-deficient mice. J Cell Biol 169, 527–538.

Nelson WJ (2009). Remodeling epithelial cell organization: transitions between front-rear and apical-basal polarity. Cold Spring Harb Perspect Biol 1, a000513.

Nitta T, Hata M, Gotoh S, Seo Y, Sasaki H, Hashimoto N, Furuse M, Tsukita S (2003). Size-selective loosening of the blood-brain barrier in claudin-5-deficient mice. J Cell Biol 161, 653–660.

Perez-Moreno M, Jamora C, Fuchs E (2003). Sticky business: orchestrating cellular signals at adherens junctions. Cell 112, 535–548.

Saitou M, Furuse M, Sasaki H, Schulzke JD, Fromm M, Takano H, Noda T, Tsukita S (2000). Complex phenotype of mice lacking occludin, a component of tight junction strands. Mol Biol Cell 11, 4131–4142.

Schneeberger EE, Lynch RD (2004). The tight junction: a multifunctional complex. Am J Physiol Cell Physiol 286, C1213–1228.

Shen L, Weber CR, Raleigh DR, Yu D, Turner JR (2011). Tight junction pore and leak pathways: a dynamic duo. Annu Rev Physiol 73, 283–309.

Shen L, Weber CR, Turner JR (2008). The tight junction complex undergoes rapid and continuous molecular remodeling at steady state. J Cell Biol 181, 683–695.

Tamura A *et al.* (2008). Megaintestine in claudin-15-deficient mice. Gastroenterology 134, 523–534.

Tamura A *et al.* (2011). Loss of claudin-15, but not claudin-2, causes Na^+ deficiency and glucose malabsorption in mouse small intestine. Gastroenterology 140, 913–923.

Tsukita S, Furuse M (2000). Pores in the wall: claudins constitute tight junction strands containing aqueous pores. J Cell Biol 149, 13–16.

Tsukita S, Furuse M, Itoh M (2001). Multifunctional strands in tight junctions. Nat Rev Mol Cell Biol 2, 285–293.

Tsukita S, Yamazaki Y, Katsuno T, Tamura A, Tsukita S (2008). Tight junction-based epithelial microenvironment and cell proliferation. Oncogene 27, 6930–6938.

Umeda K *et al.* (2006). ZO-1 and ZO-2 independently determine where claudins are polymerized in tight-junction strand formation. Cell 126, 741–754.

Van Der Wee K, Hofmann MC (1999). An in vitro tubule assay identifies HGF as a morphogen for the formation of seminiferous tubules in the postnatal mouse testis. Exp Cell Res 252, 175–185.

Van Itallie CM, Anderson JM (2006). Claudins and epithelial paracellular transport. Annu Rev Physiol 68, 403–429.

Van Itallie CM, Fanning AS, Anderson JM (2003). Reversal of charge selectivity in cation or anion-selective epithelial lines by expression of different claudins. Am J Physiol Renal Physiol 285, 1078–1084.

Van Itallie CM, Holmes J, Bridges A, Gookin JL, Coccaro MR, Proctor W, Colegio OR, Anderson JM (2008). The density of small tight junction pores varies among cell types and is increased by expression of claudin-2. J Cell Sci 121, 298–305.

Wong MH, Saam JR, Stappenbeck TS, Rexer CH, Gordon JI (2000). Genetic mosaic analysis based on Cre recombinase and navigated laser capture microdissection. Proc Natl Acad Sci USA 97, 12601–12606.

Yamamoto T, Harada N, Kano K, Taya S, Canaani E, Matsuura Y, Mizoguchi A, Ide C, Kaibuchi K (1997). The Ras target AF-6 interacts with ZO-1 and serves as a peripheral component of tight junctions in epithelial cells. J Cell Biol 139, 785–795.

Yamazaki Y, Umeda K, Wada M, Nada S, Okada M, Tsukita S, Tsukita S (2008). ZO-1- and ZO-2-dependent integration of myosin-2 to epithelial zonula adherens. Mol Biol Cell 19, 3801–3811.

Yu D, Marchiando AM, Weber CR, Raleigh DR, Wang Y, Shen L, Turner JR (2010). MLCK-dependent exchange and actin binding region dependent anchoring of ZO-1 regulate tight junction barrier function. Proc Natl Acad Sci USA 107, 8237–8241.